Design of an innovative multi-stage forming process for a complex aeronautical thin-walled part with very small radii

Wang, Yao; Lang, Lihui; Sherkatghanad, Ehsan; Nielsen, Karl Brian; Zhang, Chun

Published in:
Chinese Journal of Aeronautics

DOI (link to publication from Publisher):
10.1016/j.cja.2018.01.019

Publication date:
2018

Document Version
Publisher's PDF, also known as Version of record

Chinese Journal of Aeronautics, (2018), 31(11): 2165–2175

Chinese Society of Aeronautics and Astronautics
& Beihang University

Chinese Journal of Aeronautics

cja@buaa.edu.cn
www.sciencedirect.com

Design of an innovative multi-stage forming process for a complex aeronautical thin-walled part with very small radii

Yao WANG [a], **Lihui LANG** [a,*], **Ehsan SHERKATGHANAD** [a], **Karl Brian NIELSEN** [b], **Chun ZHANG** [c]

[a] *School of Mechanical Engineering and Automation, Beihang University, Beijing 100083, China*
[b] *Department of Materials and Production, Aalborg University, Aalborg DK-9220, Denmark*
[c] *Tianjin Tianduan Press Co., LTD, Tianjin 301700, China*

Received 2 August 2017; revised 1 September 2017; accepted 13 September 2017
Available online 31 January 2018

KEYWORDS

Double-layer sheet;
Hydroforming;
Multi-stage forming;
Small rounded corner;
Tensile-bulging effect

Abstract In this paper, an aeronautical thin-walled part with a complex geometry which has several sharp bends and curvatures in different directions was investigated. This kind of part is difficult to be manufactured only in one stage. Therefore, an innovative multi-stage active hydroforming process assisted by the rigid forming method was designed. In addition, an optimized blank geometry is obtained. In fact, the main focused point of this paper is to propose a new small radius rounded corner forming technique and analyze the mechanism. Two kinds of forming modes of changing a big rounded corner into a small one, which are related to different tangential positions of the die in the process of calibration, are analyzed theoretically. Meanwhile, the stress and strain states of the deformation region are compared. The relationships between the minimum relative radii of rounded corners I and II in the first stage and the hydraulic pressure are calculated by the bending theory. Finally, the influences of the tensile-bulging effect and the interface condition of the double-layer sheet on the forming quality of the specimen are investigated. The achieved results can make a foundation for utilizing the proposed method in forming of thin-walled parts with very small radii.

* Corresponding author.
E-mail address: lang@buaa.edu.cn (L. LANG).
Peer review under responsibility of Editorial Committee of CJA.

Production and hosting by Elsevier

1. Introduction

In recent years, the civil aircraft manufacturing technology has developed towards the overall structure of light weight, high reliability, long life, short cycle, low cost, and green advanced manufacturing technology.[1,2] Taking the A380 as a representa-

https://doi.org/10.1016/j.cja.2018.01.019
1000-9361

tive, it reflects the current status of manufacturing technology for large airliners, that is, a variety of advanced manufacturing processes are adopted to improve the performance and market competitiveness of aircraft,[3] such as the hydroforming technology adopted in this paper. Meanwhile, with the ongoing development of advanced manufacturing technologies, many more aeronautical products will be required to have a superior quality of manufacturing and are becoming more intricate. For aeronautical thin-walled sheet metal parts, they are developed in the direction of large scale, as well as high complexity and precision.[4,5] An important feature is that the radii of the rounded corners of parts are smaller and smaller for satisfying the utilization requirement under extreme weather conditions. These complex thin-walled parts with very small radii are being utilized widely, in which the inner radii are always only 1–3 times the thickness, in some cases, even less than 1 time the thickness. Besides, the surface quality requirements of the parts are high, without any obvious scratch, which will bring great difficulties to the manufacturing process.[6,7]

In terms of the above-mentioned points about complex aeronautical thin-walled parts, the sheet hydroforming technology, which uses liquid as the transmission medium of power to act on sheet metal instead of rigid dies, has shown a huge advantage for effectively improving forming accuracy and reliability of parts.[8,9] At the same time, with increasing the complexity and accuracy requirement of aeronautical thin-walled parts, many scholars have proposed some innovative technologies based on traditional sheet hydroforming, such as hydroforming with controllable radial pressure,[10] hydro-mechanical deep drawing with bilateral pressure,[11] hydroforming of sheet metal in pairs,[12] hydroforming of double-cavity with a partial die,[13] movable die sheet hydroforming,[14] and rigid-flexible coupling forming,[15] and they have made some interesting achievements. However, generally, complex aeronautical thin-walled parts need to use a multi-stage forming process. The application of hydroforming technology can always solve the key problems, such as reducing forming stages, increasing forming limits, decreasing spring-back, and improving surface quality. Kim et al.[16] proposed a multi-stage hydroforming process for a sheet pair to increase the formability of a structural part having a shape like that of an oil pan. As a result, the maximum thickness strain of the specimen has been improved more than 30%. Kong et al.[17] proposed blank multi-stage hydro-bulging by turning the active hydroforming technology upside down to improve the formability of thin-walled aeronautical corrugated parts, which included two stages as the pre-forming and reforming processes. The non-uniform wall thickness distribution and fracture defect were resolved effectively. Meng et al.[18] used hydrodynamic deep drawing combined with rigid forming to form an aeronautical wide flange box. The hydraulic pressure range was calculated, and the optimized process parameters including pre-bulging pressure, maximum pressure, and piecewise stroke were obtained. The forming stages for the part were reduced dramatically by using the hydroforming technology. Sun et al.[19] developed aluminum alloy fairing formability only by using a three-stage hydroforming process. As a result, a 50% reduction in forming stages has been achieved, compared with those of conventional rigid forming. Zhu et al.[20] proposed a schematic plan of multi-stage hydrodynamic deep drawing (HDD) assisted by conventional deep drawing (CDD). It was manufactured as a highly-qualified production by a stainless steel part with 0.4 mm thickness and complex stepped geometries.

In this paper, multi-stage active hydroforming assisted by a rigid forming method is designed innovatively for a complex aeronautical thin-walled part with very small radii. Meanwhile, preliminary blank shape and size are designed by theoretical calculation and finite element method (FEM). The main focused point of this paper is to propose a new small rounded corner forming technique based on analyzing two kinds of forming modes of changing a big rounded corner into a small one, which are related to the different tangential positions of the die in the process of calibration. Further, the influences of the tensile-bulging effect and the interface condition of the double-layer sheet on the forming quality of the specimen are investigated. The analysis is based on a combination of the theory, numerical simulation, and process test. The achieved results can make a foundation for utilizing the proposed method in forming of thin-walled parts with very small radii.

2. Process analysis

2.1. Part feature and material

In this investigation, a typical civil aircraft part with a shape and key dimensions shown in Fig. 1 was investigated. The part has a complex geometry; it has several sharp bends and curvatures in different directions. The SUS321 austenitic stainless steel alloy sheet with an initial thickness of 0.8 mm was used, and its mechanical properties are listed in Table 1. The radii of rounded corners I and III are 1.58 mm, only 1.98 times the thickness, and the radius of rounded corner II is 2.54 mm, 3.18 times the thickness. In fact, all of them are small rounded corners. Meanwhile, because R/t is much smaller than 5 (R is the radius of a rounded corner, and t is the initial thickness of the sheet), these radii are called "very small radii". In addition, due to the complex geometry, it can be recognized that the part can't be manufactured by only one-stage rigid or hydro-mechanical deep drawing. One key point of forming is precision forming for those very small rounded corners. Another is the spring-back of the part, which has been researched in a previous study by the authors,[21] and then no more details will be mentioned here.

All the experiments were carried out by a 4500-ton double-action sheet hydroforming machine, which includes a mainframe, a CNC system, and a hydraulic control system. The cavity pressure can be regulated in real time according to various designed loading paths. Meanwhile, the maximum cavity pressure can increase to 100 MPa, and the maximum BHF can reach 4000 kN. All test conditions could be set up through the software installed in the computer integrated with the press forming machine.

2.2. Process scheme design

Surface quality requirements of the part are very high, insofar as it is not allowed to have scratches with a depth greater than 0.1 mm and the surface roughness is too small. If ordinary rigid forming is utilized, the surface of the part easily will be scratched. In addition, in order to ensure the wall thickness

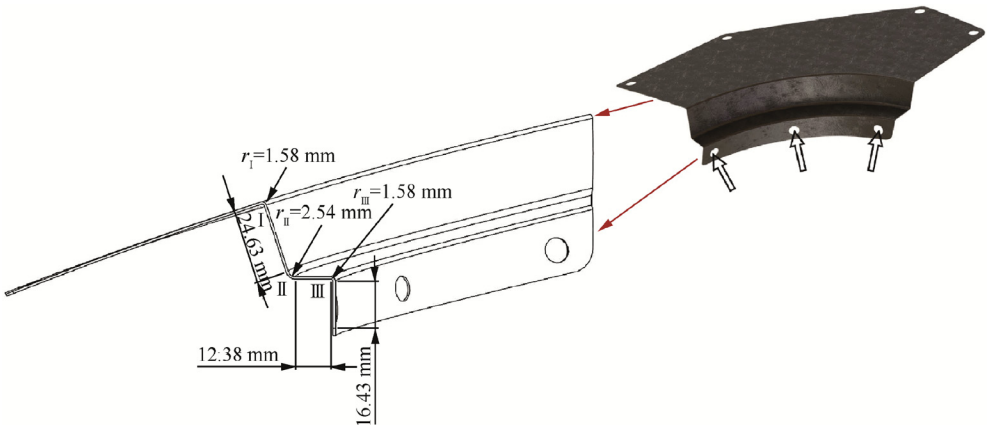

Fig. 1 Typical part with a shape and key dimensions.

Table 1 Mechanical properties of SUS321 stainless steel alloy.

Element	Value
Elastic modulus, E (MPa)	198
Yield strength, σ_s (MPa)	270
Tensile strength, σ_b (MPa)	604
Strain hardening, n	0.44
Elongation, A (%)	63

thinning rate, more than four-stage forming and shaping processes are needed. If polyurethane rubber forming is employed, because it needs to keep the pressure then the efficiency decreases, and the small rounded corner regions of the part are not easy to form, so the vertical section of the bottom (Fig. 1 at the hollow arrow position) will be broken. Therefore, high-pressure fluid medium forming (HPFMF) is introduced to make the blank deform uniformly under the action of hydraulic pressure loading, which can achieve a better forming effect, as shown in Fig. 2. Because HPFMF is generally used for closed parts, the space layout and transitional surface supplement and optimization are made for a single part. Meanwhile, the application of one die for four parts increases the uniform deformation degree of the part and improves the production efficiency and product quality.

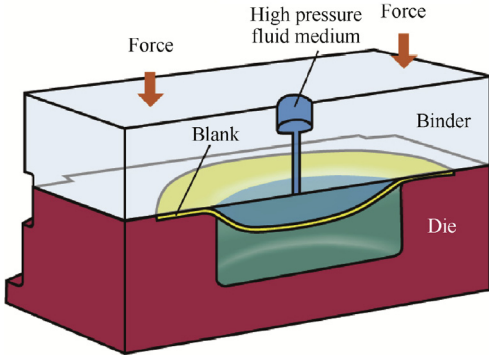

Fig. 2 Principle drawing of HPFMF.

In order to avoid the fracture and meet the requirement of precision forming for small rounded corners, preliminary blank shape and size are designed by theoretical calculation and FEM (depicted in Fig. 3). In fact, according to this approach, the non-uniform circumferential tensile stress during forming can be released effectively by cutting forks. Moreover, the stress gradient is reduced, and the formability and forming quality of rounded corner I is improved. In addition, the material flow is increased obviously by cutting a hole in the center of the blank and changing the forming mode of rounded corner II from pure hydro-bulging to compound tensile-bulging. Then the radial tensile stress in the region of rounded corner II will be decreased, and the forming quality will be improved. Finally, double-layer sheets were used in the first stage to prevent liquid leakage.

The manufacturing process of the complex aeronautical part by applying the HPFMF process is shown in Fig. 4, which has advantages of both blank uniform deformation by using HPFMF and precision forming for small rounded corners by using rigid forming (with a rubber pad in order to protect the surface of the part). Meanwhile, the proposed multi-stage forming process can decrease the number of forming steps and has not any undesirable effect on the surface quality of the part. Therefore, it is a good choice for forming of thin-walled parts with very small radii.

3. Results and analysis

3.1. Forming mechanism of rounded corner features

A two-stage manufacturing process is used for the rounded corner features I and II, and the mode is to change the radii of rounded corners from a big one to a small one. For this process, the key points are to determine the size of the rounded corner in the first stage and the forming mode of the rounded corner in the second stage.

First of all, this paper analyzes two kinds of forming modes of changing a big rounded corner into a small one in the second stage. The processes are depicted in Fig. 5, where R_I and R_{II} are the radii of rounded corners I and II obtained in the first stage, and r_I and r_{II} are the radii of final rounded corners I and II. The difference between modes one and two is related to the tangential position of the die in the process of

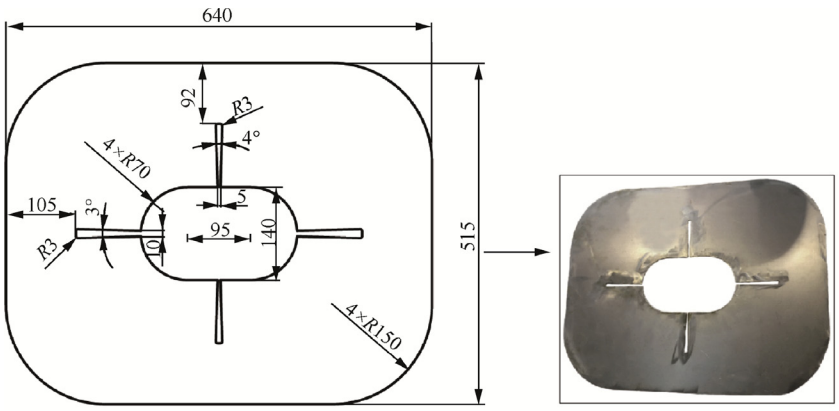

Fig. 3 Preliminary blank shape and size.

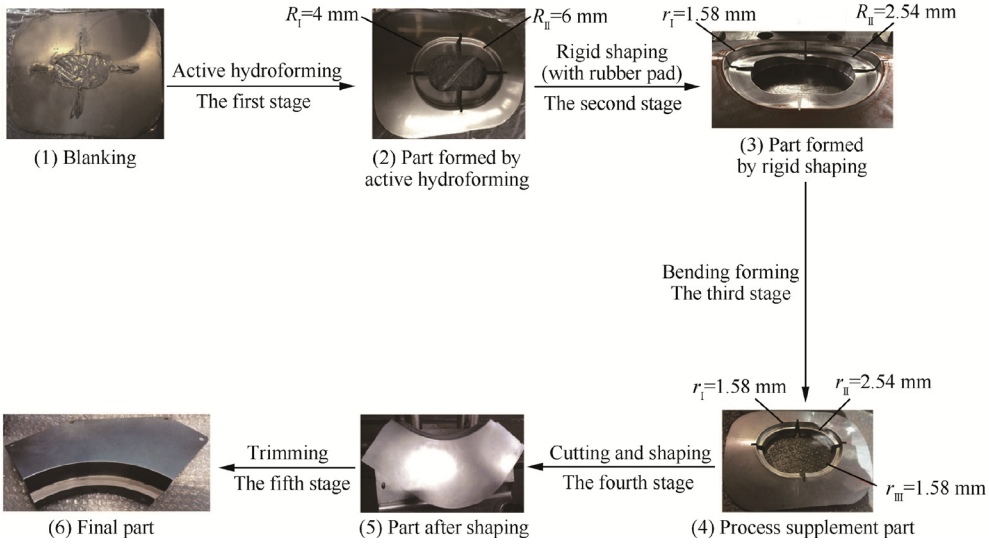

Fig. 4 Manufacturing process of the irregular complex part.

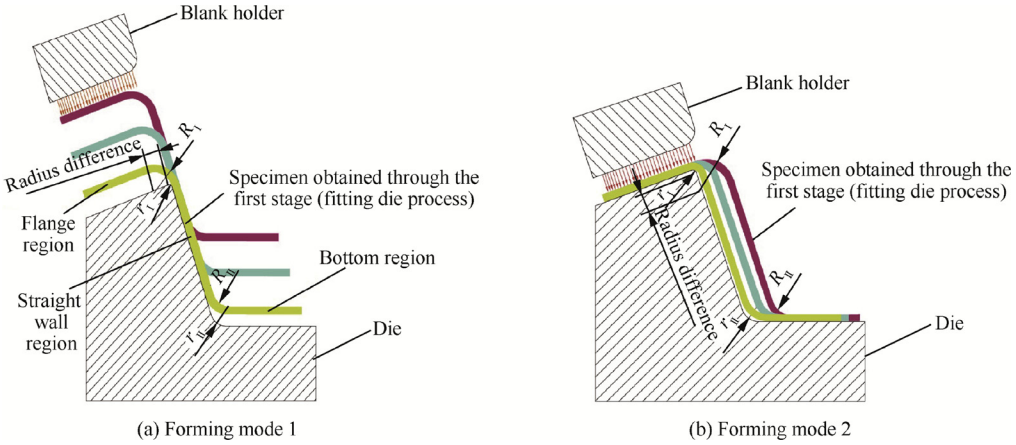

Fig. 5 Forming modes of rounded corner radii from big values to small ones in the second stage.

calibration. In the first mode, its tangent position is located in the straight wall region. Since r_I is very small, most of the upper half of rounded corner R_I is located in the die flange region, which eventually becomes the flange of the part when the blank holder is closed. After that, the punch goes down, and few of the lower half of rounded corner R_I is involved in subsequent deformation under the punch action. As it is depicted in Fig. 6, one of the imperfections in this mode is a

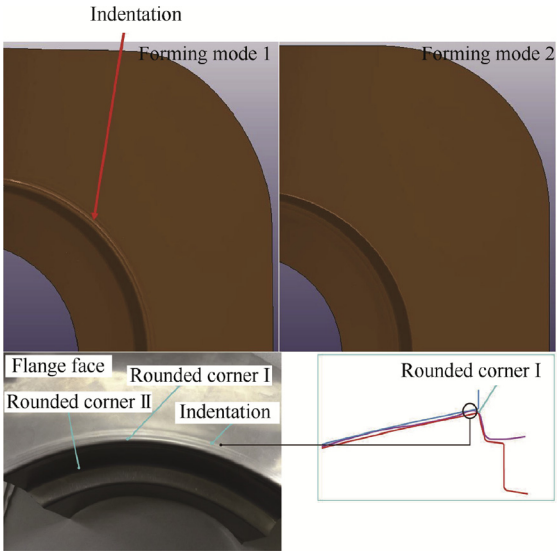

Fig. 6 Defect in the flange region produced by using forming mode one.

gap that will be observed in the flange region of the part as an indentation. It is due to the compression on the upper half of rounded corner R_I by the blank holder in the second stage. While the progress of deformation continues, the material in the straight wall region is gradually fitted to the die. Since only a small part of rounded corner R_I is involved in the deformation of the straight wall region, the radial tensile stress σ_ρ of the straight wall region increases (as shown in Fig. 7(a)), making the wall thickness of rounded corner r_I decreases (as shown in Fig. 8). Meanwhile, the blank feed amount from the straight wall region into the region of rounded corner r_{II} is insufficient, also resulting in severe wall thickness thinning of rounded corner r_{II}. In Fig. 7(a), the material flow modes from the straight wall and the bottom regions to the region of rounded corner r_{II} are depicted. The insufficient blank feed amount in this mode can be solved by a slight increase in the height of the specimen in the first stage, but the indentation of the flange (as shown in Fig. 6) cannot be eliminated in the whole conditions.

In the case of mode two, the tangential position of the die is in the flange region, so it does not cause an indentation on the specimen surface. Thereby, the forming quality will be improved. As shown in Fig. 5(b), the circumferential dimension of the preformed specimen is smaller than that of the die and calculated in this way: R_I–r_I. This will require that the formed rounded corner (R_I) in the first stage is not too large. If so, the difference in radii R_I–r_I and the circumferential strain both increase, and the thinning of the specimen will be significant. The best value of R_I is the smallest rounded corner which does not fracture in the first stage. In mode two, the forming process of rounded corner r_I is a combined forming of lateral extrusion and drawing. Based on the comprehensive influence of the lateral and tensile forces of the punch, the blank moves downward obliquely. A material storage area, in the region of rounded corner I (as shown in Fig. 7(b)), is created, which can feed the material properly for next forming of rounded corner r_{II}. Therefore, it is beneficial for forming rounded corner r_{II}. Along with the deformation progress, in the straight wall region, the blank is gradually fitted to the die. The variation of the stress state and the material flow modes from the straight wall and the bottom regions to the region of rounded corner r_{II} are depicted in Fig. 7(b). Due to the existence of the material storage area of rounded corner I, the flow of the material in the straight wall region is satisfactory as well as the blank feed amount from the straight wall region into the region of rounded corner r_{II}. It has a uniform distribution of wall thickness in rounded corner r_{II} and a good forming effect (as shown in Fig. 8). In addition, because of an increase of the circumferential stress σ_θ, the material deformation of the straight wall region is more uniform and the formability is better compared with those of mode one, which is shown in Fig. 9. Through the above analysis and experiments, it can be found that mode two is more useful to form specimens which have very small radii (r_I and r_{II}).

For the size of rounded corners I and II in the first stage, it can be designed and calculated by the plastic bending theory. In the forming process of rounded corner R_I (as shown in Fig. 10), taking the neutral layer as the boundary, the outside is a tensile stress region, and the inside is a compressive stress region. t_0 is the initial thickness of the sheet. ρ is the radius of the neutral layer.

The principal stresses of the two regions can be expressed as:

For the outside region (+):

$$\begin{cases} \sigma_1 = \frac{1+\xi}{\sqrt{1+2\xi}}\sigma_s(1 - \ln R'_I/r) + p \\ \sigma_2 = \frac{1}{\sqrt{1+2\xi}}\sigma_s[\xi - (1+\xi)\ln R'_I/r] + p \\ \sigma_3 = \frac{1+\xi}{\sqrt{1+2\xi}}\sigma_s \ln R'_I/r - p \end{cases} \quad (1)$$

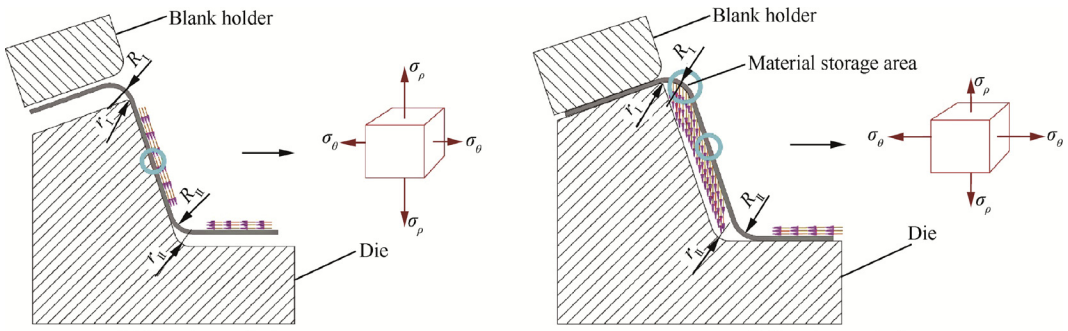

(a) Forming mode 1 (b) Forming mode 2

Fig. 7 Stress states of the straight wall region and material feed modes to form rounded corner r_{II}.

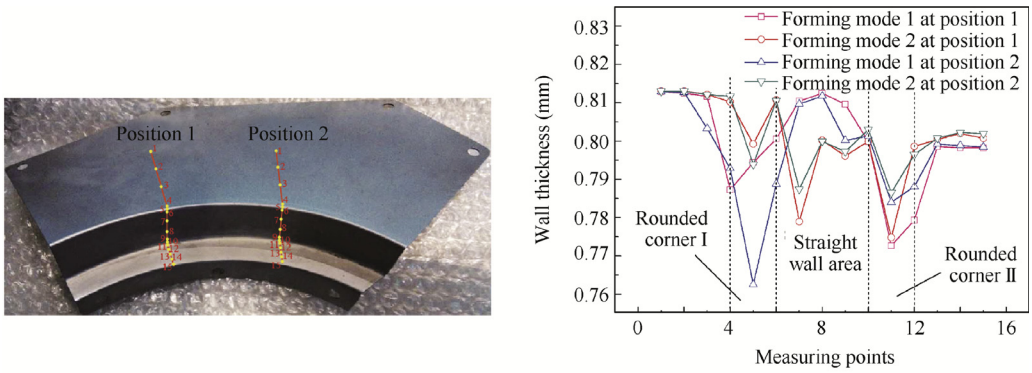

(a) Positions 1 and 2 for measuring (b) Wall thickness distributions

Fig. 8 Effects of forming modes on wall thicknesses.

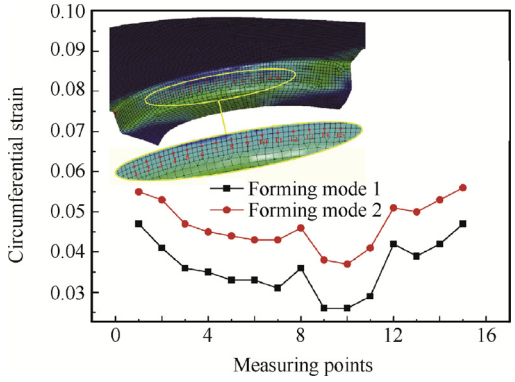

Fig. 9 Circumferential strain distribution in the straight wall region with different forming modes.

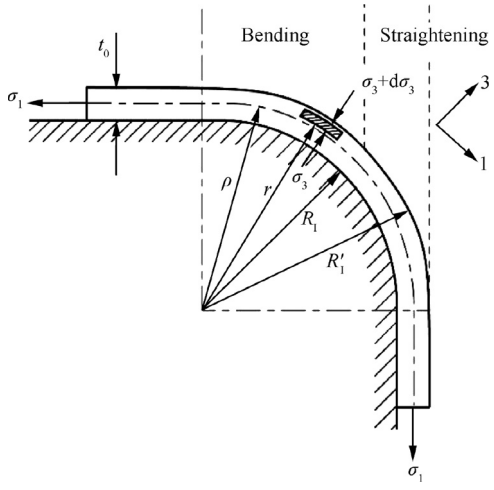

Fig. 10 Bending process of rounded corner R_I.

For the inside region (−):

$$\begin{cases} \sigma_1 = \frac{1+\xi}{\sqrt{1+2\xi}}\sigma_s(1+\ln r/R_I) - p \\ \sigma_2 = \frac{1}{\sqrt{1+2\xi}}\sigma_s[\xi + (1+\xi)\ln r/R_I] - p \\ \sigma_3 = \frac{1+\xi}{\sqrt{1+2\xi}}\sigma_s \ln r/R_I - p \end{cases} \quad (2)$$

where σ_1 is the tangential stress, σ_2 is the radial stress, and σ_3 is the transverse stress. σ_s is the yield strength. ξ is the normal anisotropy index. p is the hydraulic pressure. r is the position radius of the micro element. R_I is the internal radius of the sheet. R'_I is the outside radius of the sheet.

The average tangential stress can be expressed as:

$$\bar{\sigma}_1 = \frac{\int_{\rho}^{R'_I}\sigma_1^+ dr + \int_{R_I}^{\rho}\sigma_1^- dr}{t_0} = \frac{1+\xi}{\sqrt{1+2\xi}}\sigma_s\left(R'_I/t_0 \ln R'_I - R_I/t_0 \ln R_I - \ln\sqrt{R_I R'_I}\right) \quad (3)$$

The incidental stress caused by bending and straightening deformations is as follows:

$$\Delta\sigma_1 = \frac{\sigma_b t_0}{2R_I + t_0} \quad (4)$$

where σ_b is the tensile strength.

Meanwhile, $\sigma_3 = -p$. Therefore, the maximum equivalent stress of the bending region of rounded corner R_I can be calculated by the following formula:

$$\bar{\sigma} = \frac{\sqrt{3}}{2}\left[\frac{1+\xi}{\sqrt{1+2\xi}}\sigma_s\left(R'_I/t_0 \ln R'_I - R_I/t_0 \ln R_I - \ln\sqrt{R_I R'_I}\right) + \frac{\sigma_b t_0}{2R_I + t_0} + p\right] \quad (5)$$

In a sheet tensile test, assuming that the constitutive equation of the material satisfies the Hollomon constitutive model, the true stress and strain at fracture can be expressed as:

$$\sigma_f = K\varepsilon_f^n = -K\ln^n(1-\lambda) \quad (6)$$

where λ is the fracture section reduction rate, and $\lambda = \frac{A_0 - A_f}{A_0}$, in which A_0 is the initial cross section area at the fracture location, and A_f is the final cross section area at the fracture location. K is the strength coefficient. n is the strain-hardening exponent.

The fracture condition of rounded corner R_I can be expressed as:

$$\bar{\sigma} = \sigma_f \quad (7)$$

Therefore, the relation between the hydraulic pressure in the first stage and the minimum relative rounded corner radius φ_I is observed as follows:

$$p = \frac{2\sqrt{3}}{3} K \ln^n(1-\lambda) + \frac{1+\xi}{\sqrt{1+2\xi}}\sigma_s + \frac{(1+\xi)\sigma_s}{2\varphi_I\sqrt{1+2\xi}} + \frac{2\sigma_b}{2\varphi_I + 1} \tag{8}$$

Meanwhile, the relation between the hydraulic pressure in the first stage and the minimum relative rounded corner radius φ_{II} can be expressed by the following formula:

$$p = \frac{\sigma_s + \sigma_b}{2R_{II}} \tag{9}$$

$$\begin{cases} \varphi_I = \frac{R_I}{t_0} \\ \varphi_{II} = \frac{R_{II}}{t_0} \end{cases} \tag{10}$$

As seen in Eqs. (8)–(10), the rounded corner radii R_I and R_{II} can be designed by regulating and controlling the hydraulic pressure.

3.2. Analysis of the stress and strain in the deformation region

For the two kinds of forming modes in the second stage, the effective stress and strain distributions of the specimen at different positions are shown in Fig. 11 (the specific positions 1 and 2 are depicted in Fig. 8). It can be seen that the effective stress and strain in the regions of rounded corners I and II obtained by forming mode two are always smaller than those of forming mode one. At the selected positions 1 and 2, the maximum effective stresses in the rounded corner I region obtained by forming mode two are 782.48 MPa and 798.74 MPa, decreased by 6.98% and 3.46% respectively compared with those of forming mode one. Meanwhile, a similar situation in the rounded corner II region is that the maximum effective stresses are 613.99 MPa and 648.17 MPa respectively in forming mode two, which are also decreased by 8.49% and 0.61% respectively. For the maximum effective strain, the values of the rounded corner I region at positions 1 and 2 are 0.23 and 0.35 in forming mode one, and the values are 0.12 and 0.28 in forming mode two, which are decreased by 8.70% and 20.00% respectively. Moreover, the maximum effective strains in the rounded corner II region in forming mode two are also decreased by 1.12% and 3.77% respectively compared with those of forming mode one.

In the straight wall region, due to a bigger circumferential deformation in forming mode two, the equivalent strain and stress are both higher than those of forming mode one, but the distribution uniformities are higher than those of mode one. These further show that forming mode two can make the deformation of the straight wall region more uniform with better formability.

The evolutions of the effective stresses and strains at points A and B located in the center regions of rounded corners I and II in the forming process are shown in Fig. 12. As seen in the figures, the effective stresses and strains at points A and B increase gradually with the increase of time and the development of plastic deformation. In addition, the effective strains obtained by forming mode two are always smaller than those of mode one in the whole forming process, similar to the effective stresses except for only a few time points. No matter what kind of forming modes, the effective stress and strain at point A are always higher than those at point B. Under the two kinds of forming modes, the stress states at points A and B after forming are both biaxial tensile stress states, but the strain state at point A is a tensile-compressive state and the compressive strain value is small, while the strain state is a tensile-tensile state at point B, as shown in Figs. 13 and 14, where σ_ρ is the radial stress, σ_θ is the circumferential stress, ε_ρ is the radial strain, and ε_θ is the circumferential strain.

3.3. Influence of the tensile-bulging effect on the forming quality of rounded corner II

It is efficient to increase the flow of the material at the bottom of the specimen when making holes in the blank central region. In fact, the forming mode of rounded corner II will be changed from no-hole pure bulging to tensile-bulging compound forming. In order to satisfy and meet the requirements of the thinning rate of the wall thickness, the preforming radius of rounded corner II in the first stage can be made smaller, so it lets rounded corner II, in the second stage of the calibration process, feed adequately, and makes fracture defects hard to generate.

Set w according to this formula: $w = R/L$. Considering the influence of the hole size on the forming area, the value of L should be kept unchanged at 100 mm. The values of w are

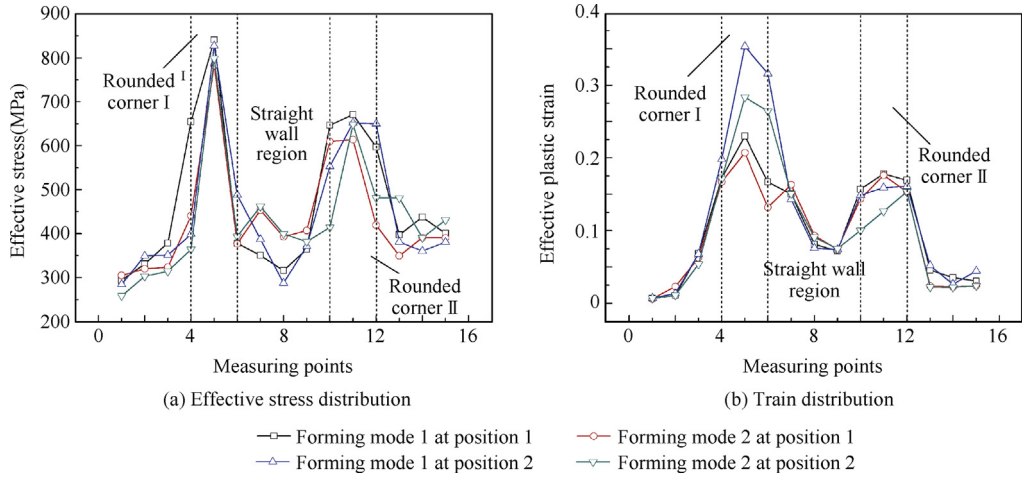

Fig. 11 Effective stress and strain distributions of the specimen at different positions.

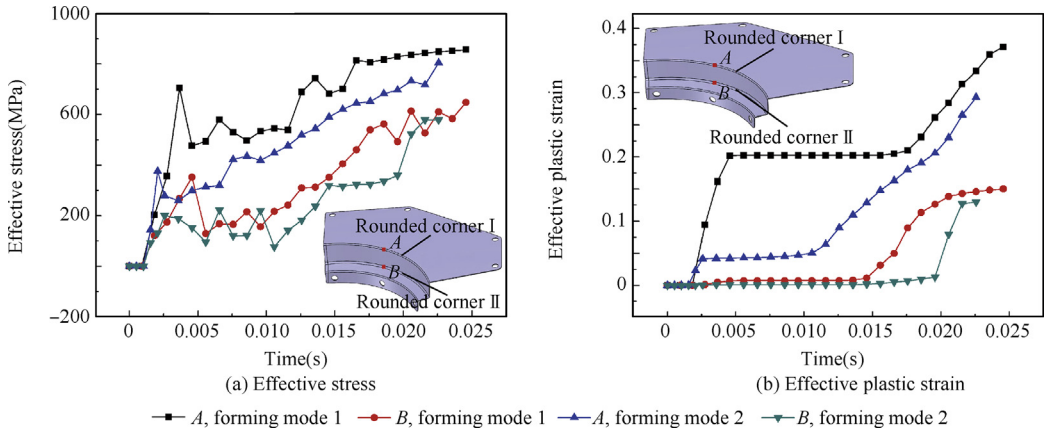

Fig. 12 Effective stress and strain evolutions at points A and B.

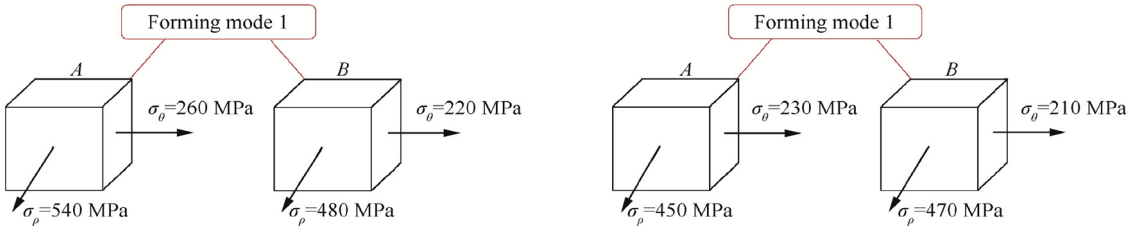

Fig. 13 Stress states at points A and B after forming.

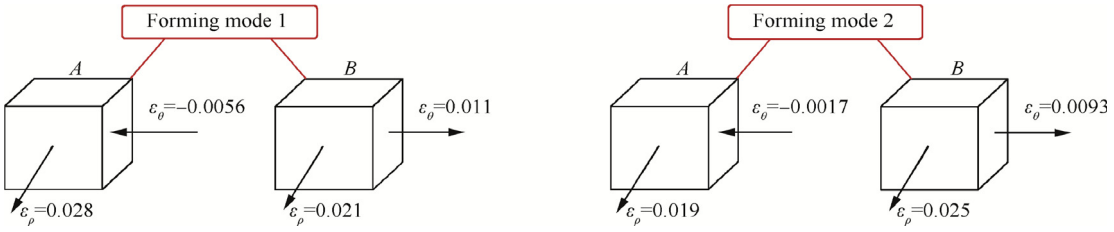

Fig. 14 Strain states at points A and B after forming.

selected as 0, 0.5, 0.7, and 0.8, respectively. The design of the hole dimension should not only meet the wall thinning rate requirements in the rounded corner region, but also have a sufficient blank side to ensure having qualified overall dimensions while the bending process is progressing in the third stage (as shown in Fig. 15), where S is the preset distance.

For different w values, the maximum thickness reduction in the rounded corner II region after the second stage and the material inflow at the hole edge in the first and second stages are shown in Fig. 16. It can be demonstrated that the wall thickness in the specimen rounded corner II region is too small, and the overall distribution uniformity is poor when $w = 0$. Due to the no-hole phenomenon at the center, the inflow volume of the

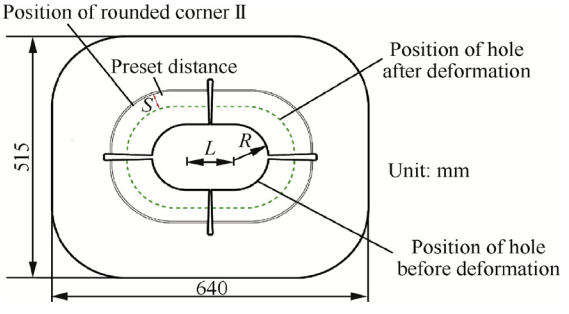

Fig. 15 Shape and dimension design for the hole.

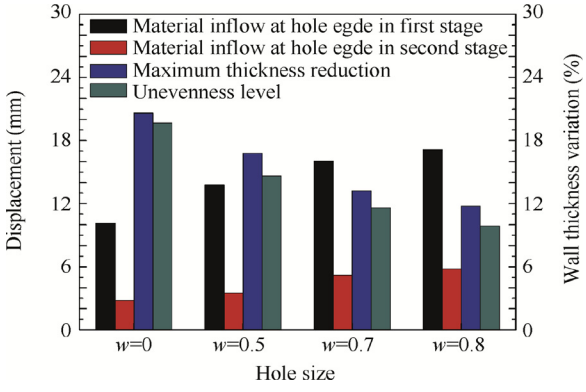

Fig. 16 Material inflow volume and wall thickness variation with different values of w.

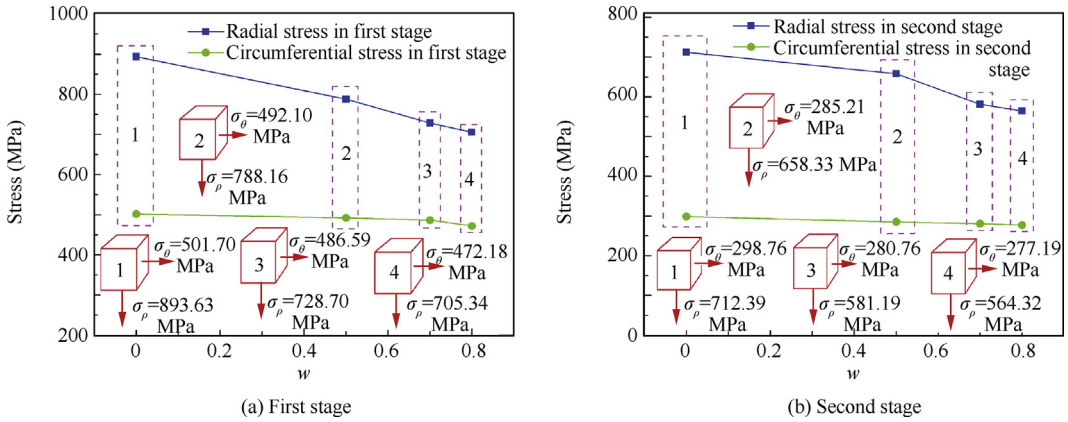

(a) First stage (b) Second stage

Fig. 17 Stress states in the rounded corner II region under different values of w.

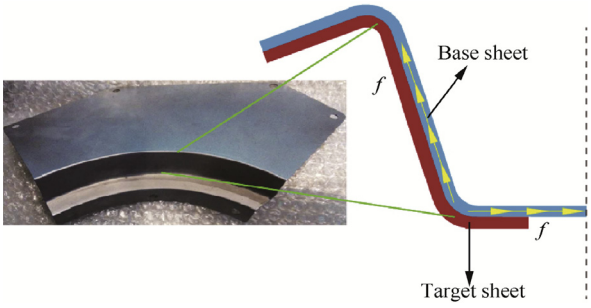

Fig. 18 Tangential friction force.

blank into the rounded corner II region is very low. Rounded corner II is formed by a large radial tensile stress, so the thinning rate of the wall thickness is significant and the formability is poor. When w = 0.8, even though the overall wall thickness keeps high, the high blank inflow volume in the central hole region causes an insufficient material edge and is unable to meet the manufacturing requirements. When w is equal to 0.5 and 0.7, the manufacturing requirements of the specimen can both be satisfied. However, when w is equal to 0.7, the wall thickness distribution uniformities of the overall and rounded corner II regions of the specimen are better, and the forming quality is superior. The stress states in the rounded corner II region under different values of w are shown in Fig. 17. It is observed that the radial tensile stresses preventing the material flow into the rounded corner region decrease with an increase of the hole size, the blank inflow is more adequate, and the formability of the rounded corner is improved quickly. However, the change of the circumferential stress in the rounded corner II region is not obvious with an increase of the hole size. Different central hole sizes can significantly change the stress and strain states of the rounded corner region and affect the final forming quality of the specimen.

3.4. Influence of the interface condition on forming of the specimen

During the active hydroforming process in the first stage, it needs to apply a base sheet in order to prevent liquid leakage, while the blank interface contact condition has a great effect on the specimen forming quality. Therefore, this section is focused on the investigation into the process through altering the friction coefficient between the blanks. In the forming process, the two blanks are kept in a sticking state under the fluid pressure condition. The tangential friction force f which is applied on the target sheet is represented in Fig. 18.

Set the friction coefficient μ between the blanks as 0, 0.05, 0.12, and 0.3, respectively. The interface friction condition has a great effect on the stress and strain distributions of the specimen. With an increase of the friction coefficient, the interface tangential friction force increases. This phenomenon causes to reduce the material flow tendency towards the

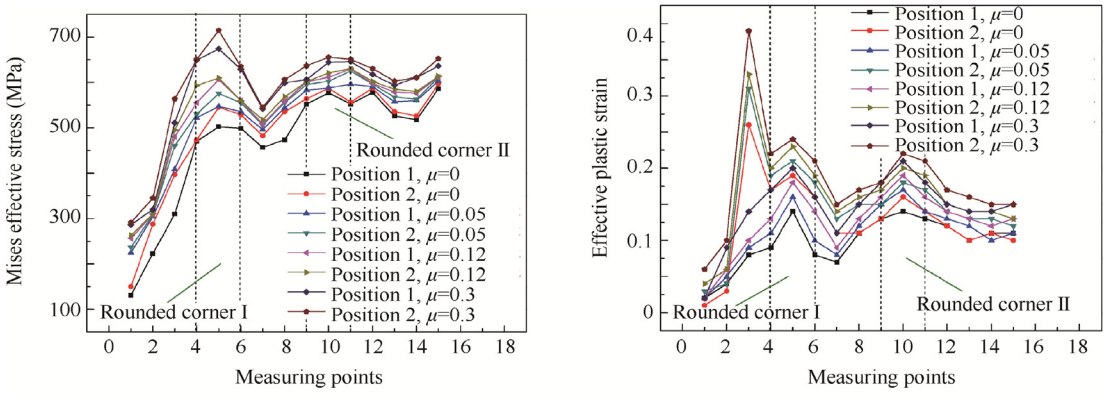

(a) Mises effective stress (b) Effective plastic strain

Fig. 19 Mises effective stress and effective plastic strain distributions under different friction coefficients.

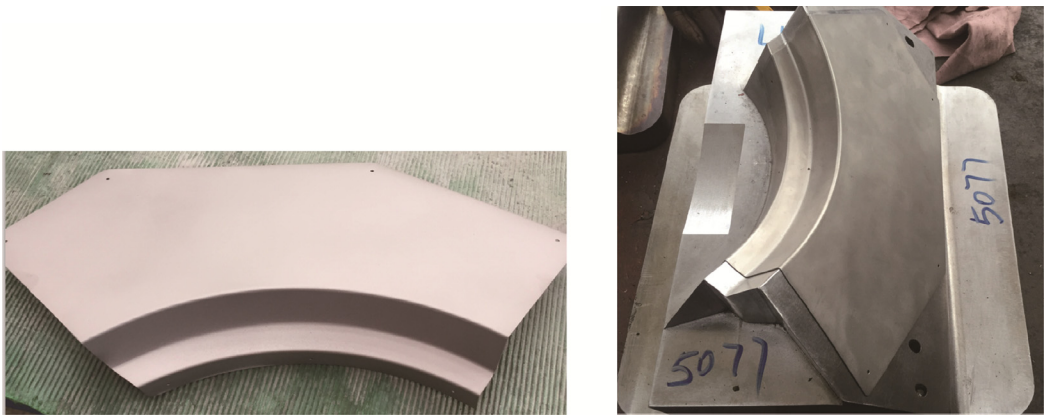

Fig. 20 Qualified specimen.

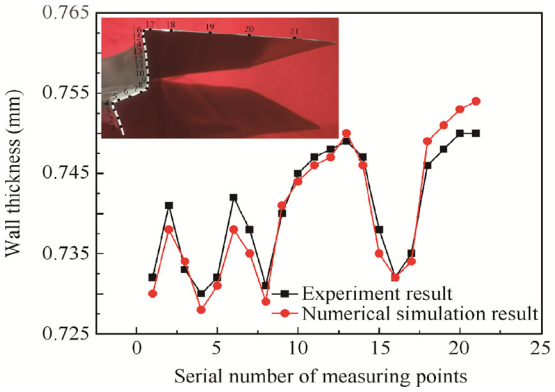

Fig. 21 Comparison of thickness distributions between experiments and FEM.

rounded corners I and II regions. It also causes to increase the radial and circumferential strains as well as an increase in the equivalent stresses in the rounded corner regions (as shown in Fig. 19(a) and (b)). It can be understood from the above-mentioned phenomenon that a suitable interface shear friction force can improve the overall deformation uniformity of the specimen, but excessive fiction would make the blank flow difficult and cause a serious thinning or even the fracture. Therefore, the specimen wall thickness distributions can be improved by controlling the interface lubricating condition.

As depicted in Fig. 20, the qualified specimen was manufactured by using the proposed multi-stage forming process and the rounded corner forming technology, which meets the tolerance and assembly requirements very well. The specimen thickness distribution was measured and compared with the result of the numerical simulation, as shown in Fig. 21. It can be found that the wall thickness distribution of the whole specimen is uniform. The results of the experiments coincide well with the simulations results.

4. Conclusions

(1) Multi-stage active hydroforming assisted by the rigid forming method was designed innovatively for a complex aeronautical part with very small radii. Preliminary blank shape and size were designed by theoretical calculation and FEM. The non-uniform circumferential tensile stress during forming can be released effectively by cutting forks, and the material flow is increased obviously by cutting a hole in the center of the blank, while the forming qualities of rounded corners I and II are improved obviously.

(2) The new rounded corner forming technique is proposed by analyzing the two kinds of forming modes in the second stage. In mode two, the tangential position of the die is in the flange region, so it does not cause an indentation on the specimen surface and is more useful to manufacture parts with very small radii compared with mode one. In addition, the stress and strain of the deformation region are obtained and then analyzed combined with FEM.

(3) Different tensile-bulging effects can significantly change the stress and strain states of the rounded corner region and affect the forming quality of the specimen. Meanwhile, the specimen wall thickness distributions can be improved by controlling the interface lubricating condition.

Acknowledgement

This study was supported by the National Science and Technology Major Project of China (No. 2014ZX04002041).

References

1. Maeno T, Mori KI, Yachi R. Hot stamping of high-strength aluminium alloy aircraft parts using quick heating. *CIRP Ann-Manuf Techn* 2017;**66**(1):269–72.
2. Zhan M, Guo K, Yang H. Advances and trends in plastic forming technologies for welded tubes. *Chin J Aeronaut* 2016;**29**(2):305–15.
3. Weiland F, Weimer C, Dumont F, Katsiropoulos CV, Pantelakis I, Sitaras I, et al. Process and cost modelling applied to manufacture of complex aerospace composite part. *Plast Rubber Compos* 2013;**42**(10):427–36.
4. Liu N, Yang H, Li H, Yan S. Plastic wrinkling prediction in thin-walled part forming process: a review. *Chin J Aeronaut* 2016;**29**(1):1–14.
5. Gao P, Li X, Yang H, Fan X, Lei Z. Improving the process forming limit considering forming defects in the transitional region in local loading forming of Ti-alloy rib-web components. *Chin J Aeronaut* 2017;**30**(3):1270–80.

6. Chu G, Liu W. Experimental observations of 5A02 aluminum alloy in electromagnetically assisted tube hydroforming. *JOM* 2013;**65**(5):599–603.
7. Swadesh KS, Kumarb DR. Effect of process parameters on product surface finish and thickness variation in hydro-mechanical deep drawing. *J Mater Process Technol* 2008;**204**(1):169–78.
8. Lu SQ, Fang J, Wang KL. Plastic deformation analysis and forming quality prediction of tube NC bending. *Chin J Aeronaut* 2016;**29**(5):1436–44.
9. Elyasi M, Bakhshi-Jooybari M, Gorji A. Mechanism of improvement of die corner filling in a new hydroforming die for stepped tubes. *Mater Des* 2009;**30**(9):3824–30.
10. Khandeparkar T, Liewald M. Hydromechanical deep drawing of cups with stepped geometries. *J Mater Process Tech* 2008;**202**(1):246–54.
11. Lin J, Zhao SD, Zhang ZY, Wang ZW. Deep drawing using a novel hydromechanical tooling. *Int J Mach Tool Manu* 2009;**49**(1):73–80.
12. Hein P, Vollertaen F. Hydroforming of sheet metal pairs. *J Mater Process Tech* 1999;**87**(1–3):154–64.
13. Siegert K, Haussermann M, Losch B, Rieger R. Recent developments in hydroforming technology. *J Mater Process Tech* 2000;**98**(2):251–8.
14. Zhang S, Zhou L, Wang Z, Xu Y. Technology of sheet hydroforming with a movable female die. *Int J Mach Tool Manu* 2003;**43**(8):781–5.
15. Zhang SH, Wang ZR, Xu Y, Wang ZT, Zhou LX. Recent developments in sheet hydroforming technology. *J Mater Process Tech* 2004;**151**(1):237–41.
16. Kim TJ, Yang DY, Han SS. Numerical modeling of the multi-stage sheet pair hydroforming process. *J Mater Process Tech* 2004;**151**(1):48–53.
17. Kong D, Lang L, Sun Z, Ruan S, Gu S. A technology to improve the formability of thin-walled aluminum alloy corrugated sheet components using hydroforming. *Int J Adv Manuf Technol* 2016;**84**(1–4):837–48.
18. Meng B, Wan M, Yuan S, Xu X, Liu J, Huang Z. Influence of cavity pressure on hydrodynamic deep drawing of aluminum alloy rectangular box with wide flange. *Int J Mech Sci* 2013;**77**(77):217–26.
19. Sun Z, Lang L, Li K, Wang Y, Zhang Q. Study on the mechanism and the suppression method of wrinkling in side wall using hydroforming of the fairing. *Int J Adv Manuf Technol* 2017;**90**(9–12):2527–35.
20. Zhu Y, Wan M, Zhou Y, Liu Q, Zheng N, Lv Z. Investigation into influence of pre-forming depth on multi-stage hydrodynamic deep drawing of thin-wall cups with stepped geometries. *Adv Mater Res* 2012;**457–458**(4):1219–22.
21. Wang Y, Lang L, Lauridsen S, Kan P. Springback analysis and strategy for multi-stage thin-walled parts with complex geometries. *J Cent South Univ* 2017;**24**(7):1582–93.